JB
Journals.ASM.org

The *Escherichia coli* Lpt Transenvelope Protein Complex for Lipopolysaccharide Export Is Assembled via Conserved Structurally Homologous Domains

Riccardo Villa,[a] Alessandra M. Martorana,[a] Suguru Okuda,[b] Louise J. Gourlay,[c] Marco Nardini,[c] Paola Sperandeo,[a] Gianni Dehò,[c] Martino Bolognesi,[c,d] Daniel Kahne,[b] Alessandra Polissi[a]

Dipartimento di Biotecnologie e Bioscienze, Università di Milano-Bicocca, Milan, Italy[a]; Department of Chemistry and Chemical Biology, Harvard University, Cambridge, Massachusetts, USA[b]; Dipartimento di Bioscienze, Università degli Studi di Milano, Milan, Italy[c]; CNR-IBF and CIMAINA, Università degli Studi di Milano, Milan, Italy[d]

Lipopolysaccharide is a major glycolipid component in the outer leaflet of the outer membrane (OM), a peculiar permeability barrier of Gram-negative bacteria that prevents many toxic compounds from entering the cell. Lipopolysaccharide transport (Lpt) across the periplasmic space and its assembly at the *Escherichia coli* cell surface are carried out by a transenvelope complex of seven essential Lpt proteins spanning the inner membrane (LptBCFG), the periplasm (LptA), and the OM (LptDE), which appears to operate as a unique machinery. LptC is an essential inner membrane-anchored protein with a large periplasm-protruding domain. LptC binds the inner membrane LptBFG ABC transporter and interacts with the periplasmic protein LptA. However, its role in lipopolysaccharide transport is unclear. Here we show that LptC lacking the transmembrane region is viable and can bind the LptBFG inner membrane complex; thus, the essential LptC functions are located in the periplasmic domain. In addition, we characterize two previously described inactive single mutations at two conserved glycines (G56V and G153R, respectively) of the LptC periplasmic domain, showing that neither mutant is able to assemble the transenvelope machinery. However, while LptCG56V failed to copurify any Lpt component, LptCG153R was able to interact with the inner membrane protein complex LptBFG. Overall, our data further support the model whereby the bridge connecting the inner and outer membranes would be based on the conserved structurally homologous jellyroll domain shared by five out of the seven Lpt components.

Lipopolysaccharide (LPS) is a unique glycolipid present in the outer layer of the outer membrane (OM) of Gram-negative bacteria (1, 2). The presence of LPS in the outer leaflet of the OM largely contributes to the permeability barrier properties exhibited by this peculiar membrane and enables Gram-negative bacteria to survive in harsh environments and to exclude several antibiotics effective against Gram-positive organisms (3). LPS biogenesis is a complex process: it involves synthesis of the different moieties at the inner leaflet of the inner membrane (IM), translocation across the IM, transport across the aqueous periplasmic space, and insertion at the outer leaflet of the OM. The LPS biosynthetic pathway is well understood (1); much less known is the mechanism by which such a large amphipathic molecule is transported across the periplasm to its final destination, the cell surface. Seven essential lipopolysaccharide transport proteins (LptABCDEFG) are required for LPS transport. They are located in three distinct cellular compartments of the *Escherichia coli* cell envelope, IM, periplasm, and OM and assemble in a transenvelope complex that bridges the IM and OM (4). The IM LptBFG complex builds an ABC transporter that provides the energy for LPS transport (5). LptF and LptG are the transmembrane (TM) components (6), whereas LptB is the IM-associated ATP binding protein (5). LptC is a small bitopic protein hosting a single TM region and a large periplasmic domain (7). LptC binds to the IM protein complex, although its association does not affect the ATPase activity of the LptBFG complex (5). At the OM, the β-barrel LptD protein and the lipoprotein LptE build up a complex responsible for LPS translocation across the OM in the final stages of assembly (8–10). LptA, the periplasmic component of the machinery (11), bridges the IM and OM interacting with LptC (12) and with the N-terminal domain of LptD (13). LptA and LptC display remarkably similar jellyroll folds despite the lack of any sequence similarity (7, 14). Interestingly, structure predictions of the LptD N-terminal periplasmic domain suggest a fold very similar to that of LptA and LptC, indicating that the bridge between the IM and OM may be built through interaction of structurally related domains (13) which are also similarly predicted for the periplasmic regions of LptF and LptG (http://zhanglab.ccmb.med.umich.edu/I-TASSER/) (12).

Coordination of Lpt protein assembly with LPS transport is crucial to prevent LPS mistargeting. Indeed, the seven Lpt proteins function in a highly concerted manner and depletion of any of them causes accumulation of the LPS at the periplasmic face of the IM (6, 11). Moreover, assembly of the Lpt bridge between the IM and OM requires formation of correct disulfide bonds in LptD (13), which in turn depends on the correct assembly of the LptDE complex (15).

We previously isolated and partially characterized two inactive *lptC* mutant alleles carrying mutations at two conserved glycines (G56 and G153) of the protein. Our results suggested that the C-terminal region of LptC is implicated in LptA binding and that

Received 1 November 2012 **Accepted** 26 December 2012
Published ahead of print 4 January 2013
Address correspondence to Alessandra Polissi, alessandra.polissi@unimib.it.
R.V. and A.M.M. contributed equally to this article.
Supplemental material for this article may be found at http://dx.doi.org/10.1128/JB.02057-12.

doi:10.1128/JB.02057-12

TABLE 1 Bacterial strains and plasmids

Bacterial strain or plasmid	Characteristic(s)[a]	Reference or source
Bacterial strains		
AM604	MC4100 ara$^+$	18
AMM04	AM604 *lptD-SPA*::*Kan*	This study
M15/pREP4	F$^-$ *lac thi mtl*/pREP4	Qiagen
BL21	F$^-$ *dcm ompT hsdS*(r_B^- m_B^-) *gal* λ (DE3)	Stratagene
DH5α	Δ(*argF-lac169*) *80dlacZ58*(M15) *glnV44*(AS) λ$^-$ *rfbD1 gyrA96 recA1 endA1 spoT1 thi-1 hsdR17*	41
FL905	AM604 Φ(*kan araC araBp-lptC*)*1*	11
C-terminal LptD-SPA	DY330 *lptD-SPA*::*Kan*	17
NR698	MC4100 *imp4213*	40
Plasmids		
pET23/42	pET23a(+) with multiple cloning sites of pET42a(+), T7 promoter; Ap^r	18
pET23/42-LptC	pET23/42-*lptC-H*	4
pET23/42-LptCG56V	pET23/42-*lptCG56V-H*	This study
pET23/42-LptCG153R	pET23/42-*lptCG153R-H*	This study
pET23/42-$MalE_{SS}$LptC	pET23/42-$malE_{SS}lptC_{\Delta 1-23}$-*H*	This study
pET23/42-$MalF_{TM}$LptC	pET23/42-$malF_{TM}lptC_{\Delta 1-23}$-*H*	This study
pET29	pET29b(+), T7 promoter; Kan^r	Novagen
pET29-$LptF_{128-252}$	pET29b-$lptF_{128-252}$-*H*	This study
pQE30	T5 promoter	Qiagen
pQEsH-*lptC*	pQE30 *sH-*$lptC_{24-191}$	12
pQEsH-*lptCG56V*	pQE30 *sH-*$lptC_{24-191}$*G56V*	This study
pQEsH-*lptCG153R*	pQE30 *sH-*$lptC_{24-191}$*G153R*	This study
pGS100	pGZ119EH derivative, contains TIR sequence downstream of *ptac*; Cm^r	36
pGS108	pGS100 *ptac-lptC-H*	36
pGS108G56V	pGS100 *ptac-lptCG56V-H*	12
pGS108G153R	pGS100 *ptac-lptCG153R-H*	12
pGS112	pGS100 *ptac-*$malF_{TM}lptC_{\Delta 1-23}$-*H*	This study
pGS114	pGS100 *ptac-*$malE_{SS}lptC_{\Delta 1-23}$-*H*	This study

[a] Antibiotic resistance to ampicillin, chloramphenicol, and kanamycin is indicated by Ap^r, Cm^r, and Kan^r, respectively.

misassembly of the Lpt components at either the IM or the OM results in LptA degradation (12). We present here a further characterization of such mutant proteins with regard to their effects on assembly of the Lpt transport complex. We find that LptCG153R interacts only with the IM LptBFG complex, whereas LptCG56V fails to interact with any of the Lpt components. By means of X-ray crystallography (the LptCG153R three-dimensional structure, here presented at 2.8-Å resolution), we establish that the G153R mutation does not induce significant structural perturbations, indicating that the observed inhibitory effects are not the result of evident conformational changes. Moreover, we show that the TM region of LptC is dispensable and not required for interaction with the IM LptBFG complex, further supporting the model whereby the bridge connecting IM and OM would be based on the interaction between the conserved structurally homologous jellyroll domains shared by five (LptACDFG) out of the seven Lpt components.

MATERIALS AND METHODS

Bacterial strains and growth conditions. The bacterial strains and plasmids are listed in Table 1. Bacteria were grown in LD medium (16). When required, 0.2% (wt/vol) L-arabinose (as an inducer of the *araBp* promoter), 0.1 mM IPTG (isopropyl-β-D-thiogalactopyranoside), 100 μg/ml ampicillin, 25 μg/ml chloramphenicol, 25 μg/ml kanamycin, 2.5 μg/ml rifampin, 50 μg/ml bacitracin, 10 μg/ml novobiocin, 0.5% (wt/vol) SDS (sodium dodecyl sulfate), and 1.0 mM EDTA were added. Solid media were prepared as described above with 1% (wt/vol) agar. The AMM04 strain (Table 1) was created by P1 transduction transferring the *lptD-SPA*::*Kan* cassette from C-terminal LptD-SPA (sequential peptide affinity) (17) in AM604 (MC4100 ara$^+$) (18).

Plasmid construction. Plasmids used in this study are listed in Table 1. The oligonucleotides used are listed in Table 2. Plasmids pGS112 and pGS114 express $MalF_{TM}$LptC-H and $MalE_{SS}$LptC-H versions of LptC, respectively, from the IPTG-inducible *ptac* promoter. $MalF_{TM}$LptC-H is composed of the first MalF transmembrane region (TM; amino acids 1 to 36) (19) fused to the periplasmic portion of LptC, starting at amino acid 24. $MalE_{SS}$LptC-H is composed of the 26-amino-acid-long signal sequence (SS) of MalE (20) fused to LptC starting at amino acid 24. The $malF_{TM}$ *lptC-H* and $malE_{SS}$ *lptC-H* chimeric genes were obtained by three-step PCR (21) using the MG1655 chromosome as the template. The final PCR products were EcoRI-HindIII digested and cloned in pGS100 cut with the same enzymes. EcoRI-HindIII inserts in pGS112 and pGS114 were verified by sequencing. Plasmids pET23/42-LptCG56V and pET23/42-LptCG153R, expressing LptCG56V and LptCG153R with a C-terminal His_8 tag from the T7 promoter, were constructed by using a QuikChange site-directed mutagenesis kit (Stratagene) with pET23/42LptC as the template and with primers listed in Table 2, as previously described (12). Plasmids pET23/42-$MalF_{TM}$LptC and pET23/42-$MalE_{SS}$LptC expressing $MalF_{TM}$LptC and $MalE_{SS}$LptC with a C-terminal His_8 tag from the T7 promoter were constructed by cloning into NdeI-XhoI-digested pET23/42 fragments obtained by PCR using pGS112 and pGS114 plasmids as the template and digested with the same enzymes. NdeI-XhoI insertions in pET23/42-$MalF_{TM}$LptC and pET23/42-$MalE_{SS}$LptC were verified by sequencing. Plasmid pQEsH-*lptCG153R* expressing His_6-$LptC_{24-191}$G153R from the T5 promoter was constructed as described above using plasmid pQEsH-*lptC* (12) as the template. The periplasmic region of LptF (residues 128 to 252) was amplified using primers AP217

TABLE 2 Oligonucleotides

Oligonucleotide name	Sequence (5′–3′)[a]	Use and/or description
AP063	gtgatcacatctagatcagtggtggtggtggtggtgAGGCTGAGTTTGTTTGTTTTG	LptC-H construction for pGS112 and pGS114; XbaI
AP204	cgagaggaattcATGGATGTCATTAAAAAGAAAC	pGS112 construction with AP063; $MalF_{TM}$LptC construction by three-step PCR with AP205; EcoRI
AP205	GTATCGTCTTTTTCGGCCATTGCGTACATTAAAACAAC	MalF-LptC hybrid primer for $MalF_{TM}$LptC construction by three-step PCR, with AP204
AP206	GTTGTTTTAATGTACGCAATGGCCGAAAAAGACGATAC	MalF-LptC hybrid primer for pGS114 construction by three-step PCR, with AP063
AP210	cgagaggaattcATGAAAATAAAAACAGGTGC	pGS114 construction with AP063; $MalE_{SS}$LptC construction by three-step PCR with AP211; EcoRI
AP211	GTATCGTCTTTTTCGGCCATGGCGAGAGCCGAGGCGGAAAAC	MalE-LptC hybrid primer for pGS114 construction by three-step PCR, with AP210
AP212	GTTTTCCGCCTCGGCTCTCGCCATGGCCGAAAAAGACGATAC	MalE-LptC hybrid primer for pGS114 construction by three-step PCR, with AP211
AP225	ggaattccatAtgAAAATAAAAACAGGTGCACGC	pET23/42-$MalF_{TM}$LptC construction with AP226; NdeI
AP226	ccgctcgagAGGCTGAGTTTGTTTGTTTTG	pET23/42-$MalF_{TM}$LptC and pET23/42-$MalE_{ss}$LptC construction with AP225 and AP270; XhoI
AP270	ggaattccatAtgGATGTCATTAAAAAGAAACATTGGTGGC	pET23/42-$MalE_{SS}$LptC construction with AP226; NdeI
AP164	GTCTATAACCCAGAA**GTG**GCACTAAGCTATCG	pET23/42-LptCG56V and pQEsH-*lptCG56V* with AP165
AP165	CGATAGCTTAGTGC**CAC**TTCTGGGTTATAGAC	pET23/42-LptCG56V and pQEsH-*lptCG56V* with AP164
AP168	CTCGTCACGTTATAC**AGA**ACAACATTTAACTC	pET23/42-LptCG153R and pQEsH-*lptCG153R* with AP168
AP169	GAGTTAAATGTTGT**TCT**GTATAACGTGACGAG	pET23/42-LptCG153R and pQEsH- *lptCG153R* with AP169
AP217	gaattccatAtgGATGAAGTGTTAGCAGAAGCG	pET29-$LptF_{128–252}$ construction with AP218; NdeI
AP218	ccgctcgagGCGCATGTCCATCTGG	pET29-$LptF_{128–252}$ construction with AP217; XhoI

[a] Uppercase letters, *E. coli* genomic sequence; underlined lowercase letters, restriction sites; boldface letters, codons mutated by site-directed mutagenesis.

and AP218 (Table 2). The resulting fragment was digested with NdeI and XhoI and ligated into pET29b (Novagen) cut with the same enzymes to give plasmid pET29-$LptF_{128–252}$.

Affinity purification and immunoprecipitation. AMM04 harboring pET23/42, pET23/42-LptC, pET23/42LptCG56V, and pET23/42-LptCG153R and AM604 harboring pET23/42-$MalF_{TM}$LptC and pET23/42-$MalE_{SS}$LptC were used in affinity purification and immunoprecipitation experiments as previously described (4) with the exception that the cells were lysed by a single cycle through a Cell Disrupter (One Shot Model by Constant Systems Ltd.) at a pressure of 22,000 lb/in^2. Immunoprecipitation protein samples were separated on a 12.5% SDS-PAGE gel. Proteins were fixed and stained with the Krypton infrared (IR) protein stain procedure (Thermo Scientific), and visualized by an Odyssey infrared imaging system (LI-COR). The identity of LptB, LptF, and LptG was confirmed by mass spectrometry (MS). Samples from affinity purification were separated on a 10% SDS-PAGE gel, electroblotted, and immunodetected using anti-Flag monoclonal antibody (Sigma-Aldrich) (1:2,000) to detect LptD-SPA, anti-His monoclonal antibodies (Sigma-Aldrich) (1:3,000) to detect wild-type and mutant LptC-H, and anti-LptA (1:2,000), anti-LptE (1:5,000), anti-LptF (1:2,000), and anti-BamA (1:10,000) polyclonal antibodies.

Cell fractionation. AM604 cells harboring pET23/42-LptC, pET23/42-LptCG56V, pET23/42-LptCG153R, pET23/42-$MalF_{TM}$LptC, and pET23/42-$MalE_{SS}$LptC were grown overnight in LD medium. Periplasmic, cytoplasmic, and inner and outer membrane fractions were prepared as described previously (22). Equal amounts of proteins from each fraction were analyzed on a 12.5% SDS-PAGE gel. The proteins were detected by immunoblotting using the anti-His monoclonal antibodies (Sigma-Aldrich). The 55-kDa IM protein that is detected by anti-LptD antibodies (11) and the OM protein BamA (18) were used as controls for confirmation of good fractionation. Membrane fractionation was performed by sucrose gradient ultracentrifugation according to published procedures (4) with the following modifications. AMM04 cells harboring pET23/42-LptC, pET23/42-LptCG56V, and pET23/42-LptCG153R were lysed by a single cycle through a Cell Disrupter (One Shot Model by Constant Systems Ltd.) at 11,000 lb/in^2. Aliquots from fractions were taken and diluted with 6× Laemmli buffer, and proteins were separated by SDS-PAGE followed by immunoblot analysis to detect the LptD-SPA tag, the 55-kDa IM protein, and LamB (1:5,000). Fraction remnants were trichloroacetic acid (TCA) precipitated (4) and analyzed by immunoblotting using anti-His monoclonal antibodies (Sigma-Aldrich) to detect wild-type and mutant LptC-H.

Expression and purification of sH-LptC, sH-LptCG56V, sH-LptCG153R, and $LptF_{128–251}$-H. An overnight culture of M15/pREP4 expressing the periplasmic domain of wild-type and mutant LptC proteins was diluted 1:100 in fresh medium and grown to the mid-logarithmic phase (optical density at 600 nm [OD_{600}], 0.6) at 37°C. Expression of sH-LptC, sH-LptCG56V, and sH-LptCG153R was induced by adding 0.5 mM IPTG, and incubation continued for 18 h at 20°C. Cells were then harvested by centrifugation (5,000 × *g*, 10 min). The cell pellet was resuspended in buffer A (50 mM NaH_2PO_4 [pH 8.0] containing 300 mM NaCl, 10 mM imidazole, and 10% glycerol), followed by 30 min of incubation at 4°C with shaking in the presence of lysozyme (0.2 mg/ml), DNase (100 μg/ml), 10 mM $MgCl_2$, and 1 mM phenylmethylsulfonyl fluoride (PMSF; Sigma-Aldrich). After disruption with one passage through a Cell Disrupter (One Shot Model by Constant Systems Ltd.) at 25,000 lb/in^2, unbroken cells were removed by centrifugation (39,000 × *g*, 30 min). The soluble proteins were purified from the supernatant by using nickel-nitrilotriacetic acid (Ni-NTA) agarose (Qiagen). The column was washed with 10 column volumes (CV) of 4% buffer B (50 mM NaH_2PO_4 [pH 8.0] containing 300 mM NaCl, 500 mM imidazole, and 10% glycerol) in buffer A. The protein was eluted by using a stepwise gradient obtained by mixing buffer B with buffer A in 5 steps (10, 20, 50, 70, and 100% buffer B). At each step, 1 CV was passed through the column. Eluate fractions were analyzed on a 12.5% polyacrylamide SDS-PAGE gel. Pooled fractions containing purified protein were dialyzed against 10 mM HEPES (pH 7.0)–50 mM NaCl for crystallization trials. Protein concentrations were determined by using a Coomassie (Bradford) assay kit (Pierce) with bovine serum albumin as the standard. For $LptF_{128–252}$-H purification, a stationary-phase culture of BL21(DE3) cells harboring pET29-$LptF_{128–252}$ (Table 1) was diluted 1:100 in fresh medium and grown to the mid-logarithmic phase at 30°C. The expression of $LptF_{128–252}$-H was induced with IPTG

as described above. Cell pellets were resuspended as described above and disrupted with one passage through a Cell Disrupter (One Shot Model by Constant Systems Ltd.) at 25,000 lb/in^2, and unbroken cells were removed by centrifugation (39,000 × *g*, 20 min). LptF protein extraction and purification were then performed as described above excepting that the Ni-NTA agarose (Qiagen) column was washed with 15 CV of 4% buffer B in buffer A. Pooled fractions containing purified protein were dialyzed against phosphate-buffered saline (PBS) buffer (137 mM NaCl, 2.7 mM KCl, 10 mM $Na_2HPO_4{\cdot}2H_2O$, 2.0 mM KH_2PO_4, pH 7.4) and processed by the Primm Company to obtain polyclonal antibodies against LptF raised in rabbit. The resulting αLptF antiserum was used at a 1:2,000 dilution.

Crystal structure analysis. Crystallization trials for sH-LptC$_{24-191}$G153R were set up in 96-well sitting drop plates (Greiner) using an Oryx 8.0 crystallization robot (Douglas Instruments), at a protein concentration of 22.3 mg/ml. Small (approximately 50-μm-diameter) crystals grew after 1 week at 20°C in a 300-nl crystallization drop containing 50% protein and 50% reservoir solution (18% polyethylene glycol 5000 monomethyl ether [PEG-MME 5K], 0.1 M sodium acetate, pH 5.5) (Stura Footprint Screen 3.1, condition 18.2; Molecular Dimensions). Crystals were cryoprotected with the same crystallization well solution supplemented with 30% glycerol, prior to cryocooling in liquid nitrogen. The crystals belong to the space group $P2_12_12_1$, with two LptCG153R chains per asymmetric unit (solvent content of 52.5%). Diffraction data were collected to 2.8-Å resolution using synchrotron radiation (ID29 beamline; ESRF, Grenoble, France) (Table 3). Raw data were processed and scaled with XDS and Scala, respectively (23, 24). The three-dimensional structure of LptCG153R was solved by molecular replacement using the structure of the wild-type protein (Protein Data Bank [PDB] code 3MY2) as a search model (7). The structure was refined using REFMAC 5.4 (25) and fitted to the generated electron density maps using Coot (26). All data were refined to satisfactory final R_{factor} and R_{free} values and stereochemical parameters (Table 3) (27, 28).

Protein structure accession number. The atomic coordinates and structure factors for LptCG153R have been deposited with the Protein Data Bank (http://www.rcsb.org) under PDB code 4B54.

RESULTS

Overexpression and subcellular localization of inactive LptC mutant proteins. *E. coli* LptC is a conserved bitopic IM protein with a single predicted N-terminal transmembrane helix (residues W7 to M24) (Expasy, http://expasy.org/) and a large soluble periplasmic domain (A25 to P191) (7). LptC interacts with the IM protein complex LptBFG and with LptA (5, 12) and bridges the IM to the OM Lpt components via LptA (13).

We previously isolated two inactive *lptC* mutant alleles carrying the single amino acid substitutions G56V and G153R, respectively (12) (Fig. 1A). Growth of LptC$^+$ depletion strain FL905 (Table 1) ectopically expressing LptCG56V is impaired under nonpermissive conditions (absence of arabinose), whereas G153R is a more severe mutation, as growth of LptC$^+$-depleted FL905 cells expressing LptCG153R is completely inhibited (12). Moreover, *in vitro* LptA binding by LptCG153R, but not by LptCG56V, is impaired, thus implicating G153 in the interaction with LptA. Both G56 and G153 are housed in two clusters of conserved residues in the periplasmic region of the protein (12). The two mutations did not seem to affect *in vivo* LptC stability, as the abundance of the mutant proteins remained constant upon inhibition of protein synthesis (see Fig. S1 in the supplemental material), or to modify the overall protein structure, as shown by circular dichroism spectra (see Fig. S2 in the supplemental material). Therefore, the phenotypes of these two mutants may depend on the specific role of the two LptC residues. To dissect their functional role, we further analyzed the properties of the two mutants.

TABLE 3 Data collection and refinement parameters for LptCG153R

Parameter	Value(s)
Data collection statistics	
Space group	$P2_12_12_1$
Unit cell dimensions	
a, *b*, *c* (Å)	48.9, 98.28, 123.56
α = β = γ (°)	90
No. of unique reflections	12,846
Avg I/σ(I)	12.9 (3.2)[a]
Completeness (%)	99.5 (99.4)
Redundancy[a]	5.1 (5.4)
R_{merge} (%)[b]	0.125 (0.722)
Refinement statistics	
Resolution range (Å)	40.0–2.8
R_{gen} (%)	22.7
R_{free} (%)[c]	28.4
No. of molecules/a.u.	2
No. of atoms	
Protein	2,043
Water	21
Acetate	1
Glycerol	1
B-factors (Å^2)	
Protein	57.1 (chain A), 68.5 (chain B)
Water	53.9
Acetate	76.3
Glycerol	62.8
RMSD	
Bond lengths (Å)	0.005
Bond angles (°)	0.904
Ramachandran plot (%)	
Favored	95.2
Allowed	100

[a] Values in parentheses represent the highest resolution shell (2.8 to 2.95 Å).
[b] $R_{merge} = \Sigma|I - (I)|/\Sigma I \times 100$, where I is the intensity of a reflection and (I) is the average intensity.
[c] R-factor $= \Sigma||F_o| - |F_c||/\Sigma|F_o| \times 100$. R_{free} was calculated from 5% of randomly selected data for cross-validation.

LptCG56V and LptCG153R were ectopically expressed in FL905, and growth of cells was tested upon IPTG induction. Overexpression of neither LptCG56V nor LptCG153R restored FL905 growth under nonpermissive conditions (Fig. 1B, −ara), suggesting that the defect of LptC single mutants is not due to a lower protein level. In line with previous observations (12), LptCG153R overexpression inhibited cell growth under permissive conditions (Fig. 1B, +ara), suggesting that the mutant protein is toxic for the cells.

To determine whether the G56V and G153R mutations could lead to mistargeting of the corresponding mutant proteins, AM604 cells expressing LptCG56V or LptCG153R mutant proteins fused to a C-terminal His$_8$ tag were fractionated, and cytoplasmic, periplasmic, IM, and OM fractions were analyzed by immunoblotting using anti-His monoclonal antibodies. Both LptCG56V and LptCG153R correctly localized in the IM (Fig. 2).

Assembly of the Lpt export machinery in G56V and G153R mutants. LptA, LptC, and the N-terminal region of LptD build the transenvelope protein bridge that connects IM and OM, providing the route for LPS transport (13). To determine whether LptC

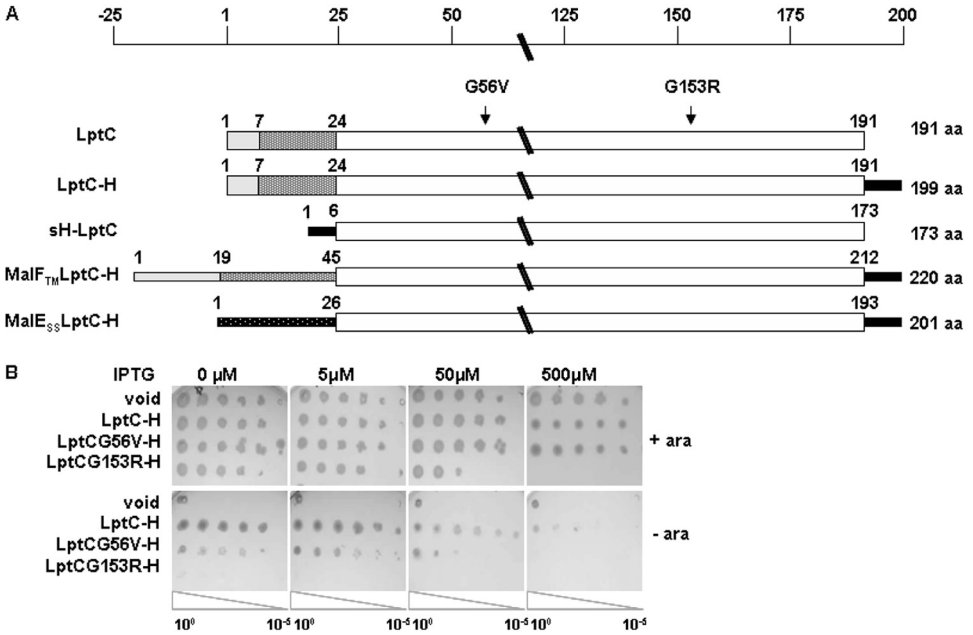

FIG 1 (A) Schematic representation of LptC and recombinant proteins. Proteins are drawn to scale, with the number of amino acids (aa) indicated on top. Rectangles of lesser height indicate a region of non-LptC origin. Gray rectangles, signal sequence for export to periplasm; gray dotted rectangles, transmembrane domain; white rectangles, LptC periplasmic domain; black rectangles, His tag; black dotted rectangle, MalE signal sequence. Arrows indicate positions of amino acid substitution. (B) Overexpression of LptCG56V-H and LptCG153R-H mutant proteins in FL905 *araBp-lptC* conditional strain. Serial 10-fold dilutions of FL905 cells transformed with pGS100 (void), pGS108 (LptC-H), pGS108G56V (LptCG56V-H), or pGS108G153R (LptCG153R-H) were replicated on agar plates supplemented with 0.2% arabinose (+ara) or left unsupplemented (−ara). The concentrations of IPTG used are indicated.

mutant proteins are able to properly assemble the Lpt machinery, we performed pulldown experiments according to the protocol developed by Chng and coworkers (4). Total membranes collected from AMM04 cells (producing a SPA-tagged LptD from the chromosomally encoded *lptD-SPA* allele) ectopically expressing C-terminally His-tagged LptC-H, LptCG56V-H, or LptCG153R-H proteins from pET23/42 vector were solubilized and affinity purified. Samples were further processed either by immunoblotting with a panel of specific antibodies (Fig. 3A) or by coimmunoprecipitation (Fig. 3B). The OM protein BamA, which is not enriched in pulldown experiments with Lpt proteins (4), was used as a loading control. As judged by the copurification profile of LptD, LptE, and LptA, neither mutant appears to be able to interact with the periplasmic component LptA and the OM complex LptD-LptE (Fig. 3A). The faint LptD and LptE signals in both LptCG56V and LptCG153R pulldown lanes appear to depend on nonspecific binding to the resin, as they are visible in the empty vector control.

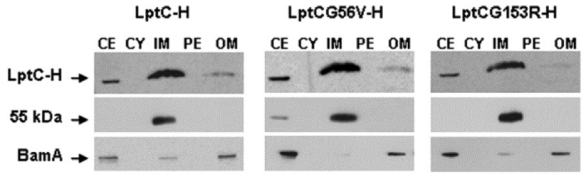

FIG 2 Subcellular localization of LptCG56V-H and LptCG153R-H mutant proteins. Crude extracts (CE) and cytoplasmic (CY), inner membrane (IM), periplasmic (PE), and outer membrane (OM) fractions from a AM604 wild-type strain harboring pET23/42-LptC, pET23/42-LptCG56V, and pET23/42-LptCG153R were prepared and analyzed by Western blotting using monoclonal α-His. The IM 55-kDa protein and the OM BamA protein are used as IM and OM markers, respectively.

On the other hand, LptCG153R copurified LptF whereas LptCG56V did not, thus indicating that the interaction with the IM LptBFG complex was impaired by the LptCG56V but not by the LptCG153R mutation. This was confirmed by coimmunoprecipitation experiments (Fig. 3B), where the LptBFG protein bands

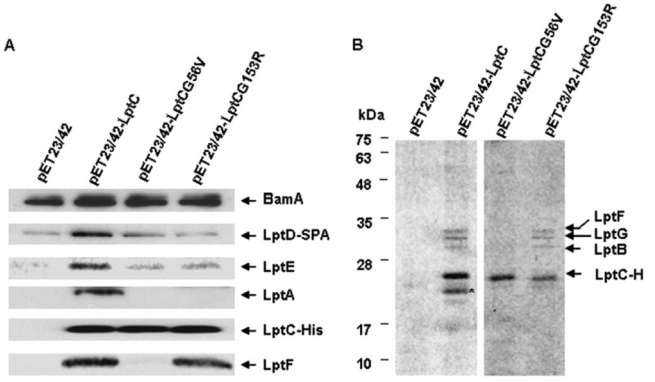

FIG 3 LptCG56V-H and LptCG153R-H mutants fail to assemble a stable transenvelope bridge. (A) Dodecyl-β-D-maltoside (DDM)-solubilized total membranes from a wild-type AMM04 strain harboring pET23/42, pET23/42-LptC, pET23/42-LptCG56V, and pET23/42-LptCG153R were affinity purified using a Talon metal affinity resin. Proteins were then fractionated by SDS-PAGE and immunoblotted with α-LptE, α-LptA, and α-LptF, with α-His to detect LptC, and with α-Flag to detect LptD-SPA. The OM BamA protein binds to the Talon metal affinity resin but is not enriched relative to the control sample and was therefore used as loading control. (B) SDS-PAGE analysis of samples (from affinity purification as described in panel A) immunoprecipitated using α-His. The identity of LptB, LptF, and LptG was confirmed by MS. The band marked with the asterisk corresponds to the immunoglobulin light chain.

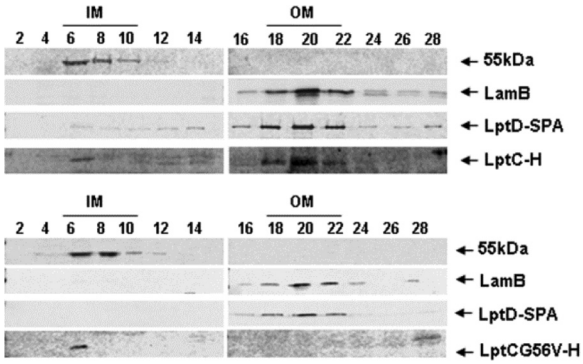

FIG 4 Sucrose gradient fractionation of AMM04 expressing LptC-H or LptCG56V-H. Cultures of AMM04 harboring pET23/42-LptC and pET23/42-LptCG56V were grown to an OD_{600} of ~0.6. Crude extracts prepared as described in Materials and Methods were fractionated by sucrose density gradient. Fractions were collected from the top of the gradient and immunoblotted using antibodies recognizing the 55-kDa protein as an IM marker and LamB as an OM marker. α-Flag and α-His were used to detect LptD-SPA and LptC His-tagged proteins, respectively.

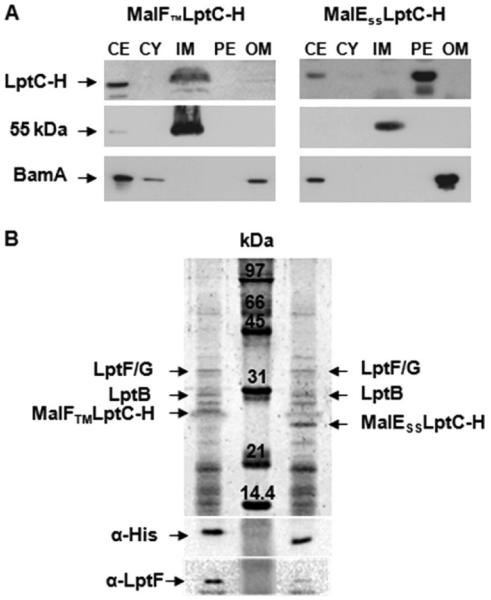

FIG 5 Subcellular localization of MalF$_{TM}$LptC-H and MalE$_{SS}$LptC-H chimeras and assembly to IM LptBFG subcomplex. (A) Crude extracts (CE) and cytoplasmic (CY), inner membrane (IM), periplasmic (PE), and outer membrane (OM) fractions from a AM604 wild-type strain harboring pET23/42-MalF$_{TM}$LptC and pET23/42-MalE$_{SS}$LptC were prepared and analyzed by Western blotting using monoclonal α-His. The IM 55-kDa protein and OM BamA are used as IM and OM markers, respectively. (B) Total membranes purified from a wild-type AM604 strain harboring pET23/42-MalF$_{TM}$LptC and pET23/42-MalE$_{SS}$LptC were affinity purified and analyzed by 10% SDS-PAGE (upper part) and by Western blotting using anti-His and anti-LptF antibodies (lower part).

were missing in the presence of the G56V mutant, but not of G153R. Therefore, LptCG56V-H fails to interact with any Lpt component, whereas LptCG153R-H can interact only with the IM complex LptBFG. The pattern of LptCG153R interactions with the Lpt components detected by the pulldown experiments described above is consistent with the inability of this mutant to bind LptA *in vitro* (12), in keeping with the observation that LptC interaction with the OM components is mediated by LptA (13). More intriguing was the phenotype of LptCG56V, which was previously shown to interact *in vitro* with LptA (12) by copurification experiments. In pulldown experiments, however, LptCG56V not only did not coimmunoprecipitate the IM components, but also did not copurify LptA and the OM LptDE complex. This discrepancy may be explained by considering that *in vivo* copurification experiments can also detect reassociation of unbound protein partners (e.g., LptA-LptC), while pulldown experiments detect only preassembled protein complexes.

Previous work demonstrated that wild-type LptC cofractionates with both IM and OM in sucrose gradient ultracentrifugation of *E. coli* membrane preparations (4). We therefore examined the sedimentation profile of LptCG56V ectopically expressed in AMM04 cells. While LptC-H cofractionated, as expected, with both IM (fractions 6 to 10) and OM (fractions 18 to 22, also containing LptD), LptCG56V was detected only in the IM fractions (Fig. 4). Since LptCG56V does not seem to form a complex with the IM LptBFG complex, its IM localization appears to depend on its TM domain only. In addition, although LptCG56V is proficient in LptA binding *in vitro*, it appears unable to associate in the transenvelope LptC-LptA-LptD bridge.

Binding of LptC to IM protein complex LptBFG occurs via the soluble periplasmic domain. To investigate the functional role of the residues composing the predicted TM region, we constructed two LptC chimeric proteins in which the TM region was replaced either by the 26-amino-acid-long signal sequence (SS 1 to 26) of MalE (MalE$_{SS}$LptC-H) (20) or by the first TM region (TM 1 to 36) of the IM-spanning protein MalF (MalF$_{TM}$LptC-H) (19). In both constructs, the C-terminal region of LptC is fused to a His$_8$ tag (Table 1 and Fig. 1A).

To determine the subcellular localization of these LptC chimeras, periplasmic, cytoplasmic, IM, and OM fractions from the wild-type AM604 strain ectopically expressing MalF$_{TM}$LptC-H and MalE$_{SS}$LptC-H from the T7 promoter at the basal level were prepared and analyzed by immunoblotting using anti-His$_6$-tag monoclonal antibodies. MalF$_{TM}$LptC-H localized in the IM fraction, whereas MalE$_{SS}$LptC-H was detected only in the periplasmic fraction, thus indicating that the MalE signal sequence promotes the secretion of LptC lacking residues 1 to 23 of the TM region into the periplasmic space (Fig. 5A).

The chimeric *malF*$_{TM}$ *lptC*$_{Δ1–23}$ and *malE*$_{SS}$ *lptC*$_{Δ1–23}$ genes cloned into the pGS100 vector under the control of the IPTG-inducible *ptac* promoter (plasmids pGS112 and pGS114, respectively; Table 1) were tested for the ability to complement the *lptC* conditional expression mutant FL905. Both MalF$_{TM}$LptC-H and MalE$_{SS}$LptC-H sustained FL905 growth under nonpermissive conditions even when the chimeric proteins were expressed at the basal level without IPTG (Fig. 6, LD −ara). To assess whether the expression of the mutant proteins lacking the wild-type LptC TM region affects OM integrity, we tested the sensitivity of FL905 cells transformed with MalF$_{TM}$LptC-H and MalE$_{SS}$LptC-H to several toxic hydrophobic compounds (29, 30). As shown in Fig. 6, FL905 LptC$^+$ depleted cells complemented by the LptC chimeras did not show increased sensitivity to any of the tested antibiotics, indicating that the OM permeability barrier was intact.

The ability of LptC chimeras to recruit the IM LptBFG protein complex was assessed by tandem affinity purification and immunoprecipitation using MalF$_{TM}$LptC-H and MalE$_{SS}$LptC-H pro-

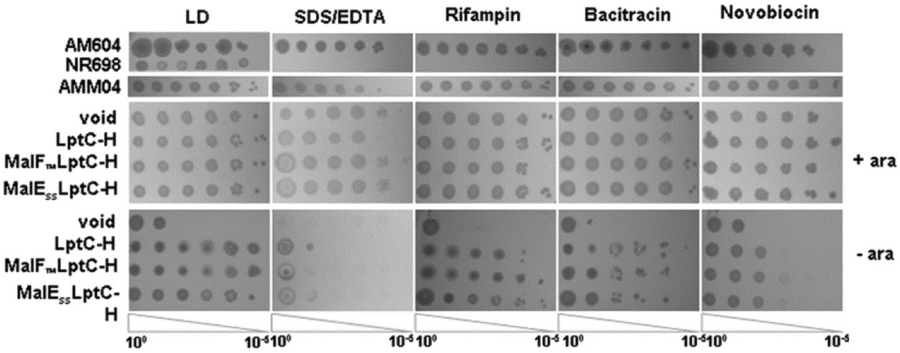

FIG 6 Ectopically expressed LptC-H, MalF$_{TM}$LptC-H, and MalE$_{SS}$LptC-H exhibit similar sensitivities to hydrophobic toxic compounds. Serial 10-fold dilutions of stationary-phase cultures of FL905 harboring pGS100 (void), pGS108 (LptC-H), pGS112 (MalF$_{TM}$LptC-H), or pGS114 (MalE$_{SS}$LptC-H) were spotted onto LD medium with 25 μg/ml chloramphenicol or onto LD medium with 25 μg/ml chloramphenicol supplemented with 0.5% SDS plus 1.0 mM EDTA, 2.5 μg/ml rifampin, 50 μg/ml bacitracin, and 10 μg/ml novobiocin in the presence (0.2% arabinose, + ara) or absence (− ara) of arabinose. Strains AM604, AMM04, and NR698 (which has a small in-frame deletion [*imp4213*] in the *lptD* gene conferring OM permeability defects to hydrophobic toxic compounds [40]) were used as controls.

teins as baits. Both chimeras copurified the IM protein complex LptBFG (Fig. 5B), suggesting that the Lpt protein machinery at the IM is correctly assembled. These results suggest that the TM domain of LptC is not required for proper assembly and functionality of the Lpt complex and that the periplasmic region of LptC is sufficient to promote binding to the IM protein complex LptBFG.

Structure of the LptCG153R periplasmic domain. The three-dimensional structure of the periplasmic region of *E. coli* LptC is known and consists of 15 antiparallel β-strands folded into a jellyroll domain (7). The G153R amino acid substitution, a lethal mutation that impairs interaction with LptA, is localized at the terminus of β-strand 12. To gain insights into the structural role of the G153 residue, we determined the crystal structure of the LptCG153R periplasmic domain (at 2.8-Å resolution), expressed as a soluble cytoplasmic protein (residues 24 to 191) lacking the transmembrane helix and with an N-terminal His$_6$ affinity tag (sH-LptCG153R) (Table 1).

sH-LptCG153R was found to be present as a dimer in the crystallographic asymmetric unit, comprising two chains (A and B), each organized into a twisted boat structure formed by the sandwiching of two β-sheets (Fig. 7). The overall fold matches closely that of the wild-type protein (Cα root mean square deviations [RMSD] of 0.8 Å and 0.5 Å for chains A and B, respectively), with

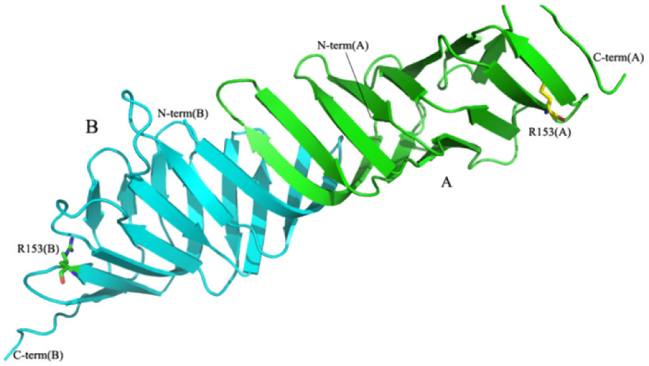

FIG 7 The crystal structure of LptCG153R. A secondary-structure cartoon representation of the sH-LptCG153R dimer present in the crystal asymmetric unit is shown. The N and C termini of monomers A (green) and B (blue) are labeled, as is the R153 mutation (sticks). This figure was generated using Mac Pymol.

electron density visible for residues 58 to 182 (chain A) and residues 59 to 184. In agreement with what has been reported for the wild-type LptC domain structure (7), the N terminus is disordered, the electron density being absent for the first 45 residues (9 belonging to the His tag region), and also for the last 7 C-terminal residues.

As illustrated by the crystal structure, the R153 mutated residue, located at the tip of β-strand 12, projects inward, roughly toward the axis of the elongated jellyroll, and is solvent accessible; despite the introduction of a large positive side chain, the LptC domain fold, which contributes to the Lpt bridge across the periplasm, is unaltered, suggesting that the lack of activity of this mutant is not related to alterations in the LptC global structure (Fig. 7). Since glycine residues are often located in conformationally flexible regions of the protein, it is possible that the G153R substitution restricts the conformational changes that would be required to allow interactions with other Lpt partners or the LPS ligand.

DISCUSSION

LPS export across the periplasm to the cell surface requires seven proteins (LptABCDEFG) that can copurify (4) and assemble into a protein bridge connecting the IM to the OM (13). Based on photo-cross-linking experiments, the architecture of the transenvelope Lpt bridge has been established to consist of a head-to-tail oligomeric assembly of the structurally homologous domains of LptC and LptA and the N-terminal region of LptD (13). According to this architecture, LptA is the central component of the machinery, with its N-terminal region contacting the C-terminal region of LptC at the IM, and its C-terminal region linking the N-terminal periplasmic region of LptD at the OM (13).

LptC is a bitopic IM protein with a single TM domain and a large periplasmic region, whose structure has been recently reported (7). LptC is essential for LPS transport, but its role in this process is unclear. It stably associates to LptA (12) and to LptBFG (5), although it does not affect the ATPase activity of this ABC transporter (5). In this context, we set out to dissect the structure-function relationships of LptC through the analysis of deletion and point mutants.

Here we demonstrate that the TM region of LptC appears to be dispensable for its function, as both a soluble periplasmic form of

LptC ($MalE_{SS}$LptC) and a chimera bearing the first TM region of MalF ($MalF_{TM}$LptC) are functional. Indeed, both chimeras complement a conditional *lptC* mutant and copurify the IM LptBFG protein complex. $MalF_{TM}$LptC appears to bind the IM protein complex more efficiently than the periplasmic $MalE_{SS}$LptC chimera (Fig. 5B), suggesting that the TM region may facilitate the interaction with LptFG. However, in $LptC^{+}$ depleted cells expressing either chimeric protein, the permeability barrier of the OM is unaffected. Therefore, LptC interaction with the IM LptBFG subcomplex appears to be mediated only by the N-terminal region of the periplasmic domain. This conclusion is further supported by the fact that the defective mutant protein LptCG56V but not LptCG153R is unable to interact with LptBFG. LptCG56V is unable to pull down LptA and the OM LptDE complex (Fig. 3A) and does not colocalize with the OM in sucrose gradient fractionation experiments (Fig. 4), although it is able to copurify LptA *in vitro* (12). This is in line with the recently proposed architecture of the LptCAD bridge that implicates the C-terminal region of LptC in binding with the N-terminal region of LptA (13). The fact that LptCG56V is not able to recruit LptA within the Lpt complex might suggest that the impaired interaction with the IM LptBFG proteins destabilizes the whole Lpt protein machinery that cannot be copurified as a single complex. Alternatively, the assembly of Lpt proteins may require an ordered/concerted process in which LptC interaction with LptBFG would be necessary for LptA recruitment. Therefore, formation of the transenvelope bridge would be inhibited in the LptCG56V mutant to prevent LPS mistargeting.

Glycine 56 is located in the linker region that connects the LptC TM segment to the periplasmic domain and is the first conserved residue from the N terminus (7). Interestingly, G56 maps at the end of one of the two disordered regions of the protein (residues 24 to 58) (7). It is not clear whether the structural effects of the G56V point mutation affect the N-terminal disordered region of the protein and/or extend to the C-terminal ordered structure immediately adjacent to it. Interaction with LptFG may occur via the unstructured linker region of LptC, in keeping with the idea that natively unfolded or partly folded proteins fold into an ordered structure upon binding partner molecules/proteins (31). Alternatively, the G56V mutation could interfere with the function of the C-terminal ordered structure immediately adjacent to the 56 site. LptC and LptA share very similar structures (7, 14) and, together with the N-terminal domain of LptD, belong to OstA structural superfamily of proteins (32, 33). Three-dimensional structure predictions reveal that the typical jellyroll fold of LptA and LptC may be present in the terminal region of LptD (13) and in the periplasmic loops of LptF and LptG (http://zhanglab.ccmb.med.umich.edu/I-TASSER/) (12). It thus appears that this structurally homologous domain, the "Lpt fold," shared by every component of the Lpt machinery, with the exception of LptB and LptE, might be the common scaffold used to build the Lpt transenvelope complex. LptA and LptC bind LPS *in vitro* (7, 34); therefore, the "Lpt fold," in addition to providing the structural element for protein-protein interaction, may also establish a continuous path across the periplasm for LPS transport from the IM to the OM.

The LptCG153R mutant displays reduced affinity for LptA *in vitro* (12), being unable to pull down LptA and the LptDE complex (Fig. 3A). G153 is a conserved residue, located at the end of β-strand 12 (7), in the proximity of the LptA-interacting residues A172 and Y182 located at the C-terminal edge (β-strand 15) in the LptC jellyroll (13). In this mutant, the small/apolar glycine 153 is substituted with arginine, a positively charged residue with high steric hindrance whose side chain faces inward toward the center of the LptC jellyroll still being solvent exposed (Fig. 7). Nevertheless, the mutant protein maintains the overall jellyroll architecture and seems to be stable *in vivo* and *in vitro* (see Fig. S1 and S2 in the supplemental material), despite the complete loss of LptC function linked to the G153R amino acid substitution; thus, the complete loss of the function of this mutant might reflect a specific role/interaction of the G153 residue. While G153 seems not to be involved in LPS binding (35), our data do not suggest an obvious explanation of how the G153R substitution impairs LptA interaction. We can speculate that the G153R mutation impairs LptA interaction by altering the electrostatics of the association interface, or by preventing the attainment of a productive conformation through steric hindrance. Isolation of an external suppressor of the $lptC_{G153R}$ mutant might help clarifying the structural basis of the LptCG153R defect. LptCG153R, which binds LptBFG but not LptA, is extremely toxic for cells, even when expressed in the presence of a wild-type copy of LptC, whereas LptCG56V is not (Fig. 1B); it is possible that LptCG153R titrates the LptBFG complex, thus preventing the formation of the complete transenvelope Lpt machine.

We previously found that LptA level decreases when the transenvelope bridge is broken because of depletion of LptD and/or LptE (12), suggesting that LptA is degraded when it is not bound to the N-terminal region of LptD. Accordingly, it has been recently demonstrated that the LptD-LptA interaction requires the correct formation of at least one native disulfide bond in LptD (15), which ultimately depends on a properly assembled LptD-LptE translocon, as a regulatory mechanism to avoid LPS mistargeting (13). LptA is also degraded when LptC is missing, or in $LptC^{+}$ depleted cells expressing a truncated and highly unstable $LptC_{\Delta 177-191}$ mutation, but not in $LptC^{+}$ depleted cells expressing LptCG153R or LptCG56V (12), despite both mutant proteins being unable to pull down LptA and LptDE (Fig. 3A). It is possible that a properly folded LptC is required for LptA folding/maturation/stability, thus explaining why LptA is stable in $LptC^{+}$ depleted cells complemented with LptCG56V and LptCG153R; in fact, we have shown that the C-terminal region of LptCG56V is proficient in LptA binding, while LptCG153R, despite being fully inactive, maintains the jellyroll fold of the wild-type protein. The strict functional interaction between LptC and LptA is reflected at the genetic level, as the coding sequences of *lptC* and *lptA* overlap by 32 nucleotides (36), suggesting a mechanism of translational coupling to ensure LptA and LptC coordinated expression. Such chromosomal organization is reminiscent of the type III secretion system SicP unieffector chaperone and its cognate effector protein SptP in *Salmonella enterica* serovar Typhimurium. Translation of the SptP effector is coupled to that of its SicP chaperone, and this prevents premature degradation of SptP and perhaps helps to target it for secretion (37). We (38) and others (34) found that overexpression of LptA under slow-growth conditions results in periplasmic localization of the protein. The accumulation of LptA in the periplasm is detrimental for the cell, likely because of the LptA tendency to oligomerize (39). Thus, LptC-LptA coexpression could be a regulative mechanism that ensures LptA association to the Lpt transport system, avoiding its mistargeting.

Taken together, the data presented in this work indicate that assembly of the Lpt machinery is finely regulated. The Lpt proteins

exploit a conserved jellyroll folded domain to build the bridge connecting IM and OM; therefore, achievement of a functional Lpt machinery in the cell must take place in a concerted manner to ensure that the component proteins recognize each other and assemble in a proper/ordered way.

ACKNOWLEDGMENTS

We thank Mohan Babu for providing the C-terminal LptD-SPA strain. We are grateful to Alberto Barbiroli (Dipartimento di Scienze Molecolari Agroalimentari, Università degli Studi di Milano) for CD analysis.

This work was supported by the Fondazione Cariplo (grant 2010.0653), the Regione Lombardia (grant 16876 SAL-18), and the Fondazione per la Ricerca sulla Fibrosi Cistica (grant FFC#13/2010), with the contribution of Donatori SMS solidale 2010.

REFERENCES

1. **Raetz CR, Whitfield C.** 2002. Lipopolysaccharide endotoxins. Annu. Rev. Biochem. **71**:635–700.
2. **Raetz CR, Guan Z, Ingram BO, Six DA, Song F, Wang X, Zhao J.** 2009. Discovery of new biosynthetic pathways: the lipid A story. J. Lipid Res. **50**(Suppl):S103–S108.
3. **Nikaido H.** 2003. Molecular basis of bacterial outer membrane permeability revisited. Microbiol. Mol. Biol. Rev. **67**:593–656.
4. **Chng SS, Gronenberg LS, Kahne D.** 2010. Proteins required for lipopolysaccharide assembly in *Escherichia coli* form a transenvelope complex. Biochemistry **49**:4565–4567.
5. **Narita S, Tokuda H.** 2009. Biochemical characterization of an ABC transporter LptBFGC complex required for the outer membrane sorting of lipopolysaccharides. FEBS Lett. **583**:2160–2164.
6. **Ruiz N, Gronenberg LS, Kahne D, Silhavy TJ.** 2008. Identification of two inner-membrane proteins required for the transport of lipopolysaccharide to the outer membrane of *Escherichia coli.* Proc. Natl. Acad. Sci. U. S. A. **105**:5537–5542.
7. **Tran AX, Dong C, Whitfield C.** 2010. Structure and functional analysis of LptC, a conserved membrane protein involved in the lipopolysaccharide export pathway in *Escherichia coli.* J. Biol. Chem. **285**:33529–33539.
8. **Braun M, Silhavy TJ.** 2002. Imp/OstA is required for cell envelope biogenesis in *Escherichia coli.* Mol. Microbiol. **45**:1289–1302.
9. **Chng SS, Ruiz N, Chimalakonda G, Silhavy TJ, Kahne D.** 2010. Characterization of the two-protein complex in *Escherichia coli* responsible for lipopolysaccharide assembly at the outer membrane. Proc. Natl. Acad. Sci. U. S. A. **107**:5363–5368.
10. **Freinkman E, Chng SS, Kahne D.** 2011. The complex that inserts lipopolysaccharide into the bacterial outer membrane forms a two-protein plug-and-barrel. Proc. Natl. Acad. Sci. U. S. A. **108**:2486–2491.
11. **Sperandeo P, Lau FK, Carpentieri A, De Castro C, Molinaro A, Dehò G, Silhavy TJ, Polissi A.** 2008. Functional analysis of the protein machinery required for transport of lipopolysaccharide to the outer membrane of *Escherichia coli.* J. Bacteriol. **190**:4460–4469.
12. **Sperandeo P, Villa R, Martorana AM, Samalikova M, Grandori R, Dehò G, Polissi A.** 2011. New insights into the Lpt machinery for lipopolysaccharide transport to the cell surface: LptA-LptC interaction and LptA stability as sensors of a properly assembled transenvelope complex. J. Bacteriol. **193**:1042–1053.
13. **Freinkman E, Okuda S, Ruiz N, Kahne D.** 2012. Regulated assembly of the transenvelope protein complex required for lipopolysaccharide export. Biochemistry **51**:4800–4806.
14. **Suits MD, Sperandeo P, Dehò G, Polissi A, Jia Z.** 2008. Novel structure of the conserved gram-negative lipopolysaccharide transport protein A and mutagenesis analysis. J. Mol. Biol. **380**:476–488.
15. **Ruiz N, Chng SS, Hiniker A, Kahne D, Silhavy TJ.** 2010. Nonconsecutive disulfide bond formation in an essential integral outer membrane protein. Proc. Natl. Acad. Sci. U. S. A. **107**:12245–12250.
16. **Sabbattini P, Forti F, Ghisotti D, Dehò G.** 1995. Control of transcription termination by an RNA factor in bacteriophage P4 immunity: identification of the target sites. J. Bacteriol. **177**:1425–1434.
17. **Babu M, Aoki H, Chowdhury WQ, Gagarinova A, Graham C, Phanse S, Laliberte B, Sunba N, Jessulat M, Golshani A, Emili A, Greenblatt JF, Ganoza MC.** 2011. Ribosome-dependent ATPase interacts with conserved membrane protein in *Escherichia coli* to modulate protein synthesis and oxidative phosphorylation. PLoS One **6**:e18510.
18. **Wu T, McCandlish AC, Gronenberg LS, Chng SS, Silhavy TJ, Kahne D.** 2006. Identification of a protein complex that assembles lipopolysaccharide in the outer membrane of *Escherichia coli.* Proc. Natl. Acad. Sci. U. S. A. **103**:11754–11759.
19. **Oldham ML, Khare D, Quiocho FA, Davidson AL, Chen J.** 2007. Crystal structure of a catalytic intermediate of the maltose transporter. Nature **450**:515–521.
20. **Bedouelle H, Bassford PJ, Jr, Fowler AV, Zabin I, Beckwith J, Hofnung M.** 1980. Mutations which alter the function of the signal sequence of the maltose binding protein of *Escherichia coli.* Nature **285**:78–81.
21. **Chaveroche MK, Ghigo JM, d'Enfert C.** 2000. A rapid method for efficient gene replacement in the filamentous fungus Aspergillus nidulans. Nucleic Acids Res. **28**:E97.
22. **Oliver DB, Beckwith J.** 1982. Regulation of a membrane component required for protein secretion in *Escherichia coli*. Cell **30**:311–319. 6751561.
23. **Evans P.** 2006. Scaling and assessment of data quality. Acta Crystallogr. D Biol. Crystallogr. **62**:72–82.
24. **Kabsch W.** 2010. Integration, scaling, space-group assignment and post-refinement. Acta Crystallogr. D Biol. Crystallogr. **66**:133–144.
25. **Murshudov GN, Vagin AA, Dodson EJ.** 1997. Refinement of macromolecular structures by the maximum-likelihood method. Acta Crystallogr. D Biol. Crystallogr. **53**:240–255.
26. **Emsley P, Cowtan K.** 2004. Coot: model-building tools for molecular graphics. Acta Crystallogr. D Biol. Crystallogr. **60**:2126–2132.
27. **Lovell SC, Davis IW, Arendall WB, III, de Bakker PI, Word JM, Prisant MG, Richardson JS, Richardson DC.** 2003. Structure validation by Calpha geometry: phi,psi and Cbeta deviation. Proteins **50**:437–450.
28. **Davis IW, Leaver-Fay A, Chen VB, Block JN, Kapral GJ, Wang X, Murray LW, Arendall WB, III, Snoeyink J, Richardson JS, Richardson DC.** 2007. MolProbity: all-atom contacts and structure validation for proteins and nucleic acids. Nucleic Acids Res. **35**:W375–W383.
29. **Ruiz N, Silhavy TJ.** 2005. Sensing external stress: watchdogs of the Escherichia coli cell envelope. Curr. Opin. Microbiol. **8**:122–126.
30. **Chimalakonda G, Ruiz N, Chng SS, Garner RA, Kahne D, Silhavy TJ.** 2011. Lipoprotein LptE is required for the assembly of LptD by the beta-barrel assembly machine in the outer membrane of *Escherichia coli.* Proc. Natl. Acad. Sci. U. S. A. **108**:2492–2497.
31. **Dyson HJ, Wright PE.** 2002. Coupling of folding and binding for unstructured proteins. Curr. Opin. Struct. Biol. **12**:54–60.
32. **Bos MP, Robert V, Tommassen J.** 2007. Biogenesis of the gram-negative bacterial outer membrane. Annu. Rev. Microbiol. **61**:191–214.
33. **Finn RD, Tate J, Mistry J, Coggill PC, Sammut SJ, Hotz HR, Ceric G, Forslund K, Eddy SR, Sonnhammer EL, Bateman A.** 2008. The Pfam protein families database. Nucleic Acids Res. **36**:D281–D288.
34. **Tran AX, Trent MS, Whitfield C.** 2008. The LptA protein of *Escherichia coli* is a periplasmic lipid A-binding protein involved in the lipopolysaccharide export pathway. J. Biol. Chem. **283**:20342–20349.
35. **Okuda S, Freinkman E, Kahne D.** 2012. Cytoplasmic ATP hydrolysis powers transport of lipopolysaccharide across the periplasm in *E. coli.* Science **338**:1214–1217.
36. **Sperandeo P, Pozzi C, Dehò G, Polissi A.** 2006. Non-essential KDO biosynthesis and new essential cell envelope biogenesis genes in the *Escherichia coli yrbG-yhbG* locus. Res. Microbiol. **157**:547–558.
37. **Button JE, Galan JE.** 2011. Regulation of chaperone/effector complex synthesis in a bacterial type III secretion system. Mol. Microbiol. **81**:1474–1483.
38. **Sperandeo P, Cescutti R, Villa R, Di Benedetto C, Candia D, Dehò G, Polissi A.** 2007. Characterization of *lptA* and *lptB*, two essential genes implicated in lipopolysaccharide transport to the outer membrane of *Escherichia coli.* J. Bacteriol. **189**:244–253.
39. **Merten JA, Schultz KM, Klug CS.** 2012. Concentration-dependent oligomerization and oligomeric arrangement of LptA. Protein Sci. **21**:211–218.
40. **Ruiz N, Falcone B, Kahne D, Silhavy TJ.** 2005. Chemical conditionality: a genetic strategy to probe organelle assembly. Cell **121**:307–317.
41. **Hanahan D.** 1983. Studies on transformation of *Escherichia coli* with plasmids. J. Mol. Biol. **166**:557–580.